Diffraction by a rigid barrier with a soft or perfectly absorbent end face

P. McIver

Department of Mathematical Sciences, Loughborough University,

Loughborough, Leics, LE11 3TU, UK

A.D. Rawlins

Department of Mathematics & Statistics, Brunel University,

Uxbridge, Middx, UB8 3PH, UK

Abstract

The reduction of noise levels in the shadow region of a rigid barrier of finite thickness is considered when the end face of the barrier is lined with either a soft or a perfectly absorbent material. Solutions, obtained by the method of matched asymptotic expansions, are given for both a semi-infinite barrier and for a finite length barrier placed on a rigid plane. Comparisons are made with existing solutions for barriers that have a rigid end face.

1 Introduction

Noise reduction by barriers is a common sense measure of environmental protection in heavily built-up areas. In particular, noise from motorways, railways and airports can be shielded by a barrier which intercepts the line-of-sight from the source to the receiver. The acoustic field in the shadow region of a barrier (when transmission through the barrier is negligible) is due to diffraction at the edge alone.

The design of such noise barriers should meet two important requirements: namely that they are effective noise attenuators and that their construction and maintenance should be economical. The latter requirement is not difficult to appreciate when one considers the miles of motorway which run through built-up areas. One possible economical barrier construction is to have a rigid barrier (hence eliminating transmitted noise) of cheap material which is robust, and not necessarily a good attenuator of edge diffracted noise, and to cover the surface of the barrier with a sound absorbing lining which is a good attenuator of sound. The provision of a barrier covered completely with an absorbing lining presents several difficulties, among them the costs of construction and maintenance. However, since diffraction phenomena are governed by conditions at the diffracting edge, it would be more economic to cover the region only in the immediate vicinity of the edge with sound absorbing material. Butler [1] found, when dealing with thin barriers, reasonable agreement with the experimental results of Maekawa[2]. All practical barriers have thickness, and the object of the present work is to consider the qualitative effect of the thickness of a noise barrier, with local absorbency at the edge, on the sound attenuation in the shadow region of the barrier. The direct solution of this problem with the absorbent type boundary condition on the finite absorptive end face is very difficult and becomes involved in very complicated mathematics. To simplify matters we shall replace the absorptive boundary condition by a perfectly soft boundary condition. However, as pointed out by Jones [3], this barrier would be expected to produce much higher levels of noise attenuation, in the shadow region of the barrier, than an absorbent end-face barrier. A compromise which gives some realistic quantitative estimate of the attenuation due to an absorbent region on a barrier is to use the concept of a 'perfectly absorbing' end surface (Butler [1], Jones [3], Rawlins [4]). This is obtained by adding the solutions (for the same incident wave) for a completely rigid thick half-plane, Crighton & Leppington [5], and the rigid thick half-plane with a soft end face and divided by two. As a further practical application we shall also include the effect of such a barrier of finite length placed on rigid, flat ground.

The solution for the canonical problem of a thick half-plane with a soft edge will be obtained by an application of the method of matched asymptotic expansions. This canonical problem will be formulated and solved in §§2-3. In §4, the effect of a rigid ground, with a

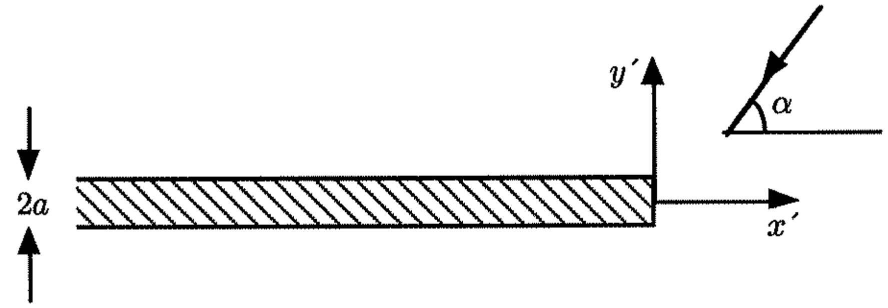

Figure 1: Definition sketch for wave scattering by semi-infinite barrier.

finite thick barrier perpendicularly emplaced, will be considered. Throughout the problems are taken to be purely two dimensional. In §5, graphical results will be given and comparisons made with a thin rigid barrier.

2 Formulation for the semi-infinite barrier

A plane wave of wavenumber k and frequency ω is incident at an angle α to a semi-infinite barrier of constant thickness $2a$. Cartesian coordinates (x', y') are chosen with origin in the flat end of the barrier as illustrated in figure 1. Assuming that a time factor $\mathrm{e}^{-i\omega t}$ has been removed, the total velocity potential describing the flow is written

$$\phi_T' = \phi_I' + \phi' \tag{1}$$

where the incident wave potential

$$\phi_I' = \exp\left[-ik(x'\cos\alpha + y'\sin\alpha)\right]. \tag{2}$$

Solutions of the scattering problem are sought that satisfy a 'soft' condition on the barrier end face,

$$\phi_T' = 0 \quad \text{on} \quad x' = 0,\ |y'| < a, \tag{3}$$

and a 'hard' condition on the long sides of the barrier,

$$\frac{\partial \phi_T'}{\partial y'} = 0 \quad \text{on} \quad |y'| = a,\ x' < 0. \tag{4}$$

The scattered field ϕ' must also satisfy a radiation condition specifying outgoing waves.

The geometry and boundary conditions to be applied are symmetric about $y' = 0$ so that the scattered potential ϕ' may be split into symmetric and antisymmetric parts as

$$\phi'(x', y') = \phi'_S(x', y') + \phi'_A(x', y'), \quad y' \geq 0. \tag{5}$$

The field for $y' < 0$ is then defined through

$$\phi'_S(x', -y') = \phi'_S(x', y') \quad \text{and} \quad \phi'_A(x', -y') = -\phi'_A(x', y') \tag{6}$$

so that

$$\frac{\partial \phi'_S}{\partial y'} = 0 \quad \text{and} \quad \phi'_A = 0 \quad \text{on} \quad y' = 0,\ x' > 0. \tag{7}$$

The incident wave potential also may be split into symmetric and antisymmetric parts as

$$\phi'_I = \mathrm{e}^{-ikx'\cos\alpha}\left[\cos(ky'\sin\alpha) - i\sin(ky'\sin\alpha)\right]. \tag{8}$$

As a consequence of these relations it is sufficient to consider only the region $y' \geq 0$.

Throughout it will be assumed that the barrier thickness $2a$ is much smaller than the wavelength $2\pi/k$ so that $\epsilon = ka \ll 1$. The method of matched asymptotic expansions will be used to obtain the solutions as perturbation series in the small parameter ϵ.

2.1 Symmetric problem

The symmetric part of the scattered potential, defined through equations (5–7), is a solution of the Helmholtz equation and, as a consequence of the above definitions, satisfies the boundary conditions

$$\begin{aligned} \frac{\partial \phi'_S}{\partial y'} &= -\frac{\partial}{\partial y'}\left[\mathrm{e}^{-ikx'\cos\alpha}\cos(ky'\sin\alpha)\right] \\ &= k\sin\alpha\,\mathrm{e}^{-ikx'\cos\alpha}\sin(ka\sin\alpha) \quad \text{on} \quad y' = a,\ x' < 0 \end{aligned} \tag{9}$$

for the barrier sides, and

$$\phi'_S = -\cos(ky'\sin\alpha) \quad \text{on} \quad x' = 0,\ 0 < y' < a, \tag{10}$$

for the barrier tip. The symmetry condition in (7) and the radiation condition are assumed to hold throughout but will not be explicitly stated.

For the solution by matched asymptotic expansions, the flow region is divided into two regions. These are an inner region around the barrier tip to radial distances $r' \ll k^{-1}$ and an outer region at distances $r' \gg a$. The length scale of the outer region flow is k^{-1} and non-dimensional coordinates are defined by

$$x = kx' \quad \text{and} \quad y = ky'; \tag{11}$$

plane polar coordinates (r, θ) defined by

$$x = r\cos\theta \quad \text{and} \quad y = r\sin\theta \tag{12}$$

will also be used. With this change of variables, the outer potential $\phi_S(x, y) \equiv \phi'_S(x', y')$ satisfies the field equation

$$\left(\nabla^2 + 1\right)\phi_S = 0, \tag{13}$$

and the boundary condition

$$\frac{\partial \phi_S}{\partial y} = \sin\alpha\,\mathrm{e}^{-ix\cos\alpha}\sin(\epsilon\sin\alpha) \quad \text{on} \quad y = \epsilon,\ x < 0 \tag{14}$$

on the barrier sides. Under the assumption $ka \ll 1$, the barrier thickness is not discernible on the length scale of the outer region so that the boundary condition (10) is not applied in this region. The boundary condition (14) may be transferred to $y = 0$ by Taylor series expansion so that

$$\frac{\partial \phi_S}{\partial y} + \epsilon\frac{\partial^2 \phi_S}{\partial y^2} = \epsilon\sin^2\alpha\,\mathrm{e}^{-ix\cos\alpha} + O\left(\epsilon^2\right) \quad \text{on} \quad y = 0,\ x < 0. \tag{15}$$

For the inner region with length scale a, suitable non-dimensional coordinates are

$$X = x'/a \quad \text{and} \quad Y = y'/a, \tag{16}$$

and plane polar coordinates (R, θ) defined by

$$X = R\cos\theta \quad \text{and} \quad Y = R\sin\theta \tag{17}$$

will also be used. The inner potential $\psi_S(X, Y) \equiv \phi'_S(x', y')$ satisfies the field equation

$$\left(\nabla^2 + \epsilon^2\right)\psi_S = 0. \tag{18}$$

In the inner region both of the boundary conditions (9-10) must be applied and in terms of the inner variables these are

$$\frac{\partial \psi_S}{\partial Y} = \epsilon \sin\alpha\, \mathrm{e}^{-i\epsilon X\cos\alpha} \sin(\epsilon Y \sin\alpha) = \epsilon^2 \sin^2\alpha + O(\epsilon^3) \quad \text{on} \quad Y = 1,\ X < 0 \tag{19}$$

and

$$\psi_S = -\cos(\epsilon Y \sin\alpha) = -1 + \tfrac{1}{2}\epsilon^2 Y^2 \sin^2\alpha + O(\epsilon^4) \quad \text{on} \quad X = 0,\ Y < 1. \tag{20}$$

2.2 Antisymmetric problem

The antisymmetric part of the scattered potential, defined through equations (5–7), is a solution of the Helmholtz equation and, as a consequence of the above definitions, satisfies the boundary conditions

$$\begin{aligned} \frac{\partial \phi_A'}{\partial y'} &= -\frac{\partial}{\partial y'}\left[-\mathrm{e}^{-ikx'\cos\alpha}\, i\sin(ky'\sin\alpha)\right] \\ &= ik\sin\alpha\, \mathrm{e}^{-ikx'\cos\alpha}\cos(ka\sin\alpha) \quad \text{on} \quad y' = a,\ x' < 0, \end{aligned} \tag{21}$$

for the barrier sides, and

$$\phi_A' = i\sin(ky'\sin\alpha) \quad \text{on} \quad x' = 0,\ 0 < y' < a, \tag{22}$$

for the barrier tip. The antisymmetry condition in (7) and the radiation condition are assumed to hold throughout but will not be explicitly stated.

The flow region is divided into two regions as described in §2.1 and scaled variables introduced as in equations (11) and (16). With this change of variables, the outer potential $\phi_A(x, y) \equiv \phi_A'(x', y')$ satisfies the field equation

$$\left(\nabla^2 + 1\right)\phi_A = 0, \tag{23}$$

and the boundary condition

$$\frac{\partial \phi_A}{\partial y} = i\sin\alpha\, \mathrm{e}^{-ix\cos\alpha}\cos(\epsilon\sin\alpha) \quad \text{on} \quad y = \epsilon,\ x < 0 \tag{24}$$

on the barrier sides. Under the assumption $ka \ll 1$, the barrier thickness is not discernible on the length scale of the outer region so that the boundary condition (22) is not applied in this region. The boundary condition (24) may be transferred to $y = 0$ by Taylor series expansion so that

$$\frac{\partial \phi_A}{\partial y} + \epsilon \frac{\partial^2 \phi_A}{\partial y^2} = i \sin\alpha\, \mathrm{e}^{-ix\cos\alpha} + O(\epsilon^2) \quad \text{on} \quad y = 0,\ x < 0. \tag{25}$$

The inner potential $\psi_A(X, Y) \equiv \phi'_A(x', y')$ satisfies the field equation

$$\left(\nabla^2 + \epsilon^2\right) \psi_A = 0. \tag{26}$$

In the inner region both of the boundary conditions (21–22) must be applied and in terms of the inner variables these are

$$\begin{aligned} \frac{\partial \psi_A}{\partial Y} &= i\epsilon \sin\alpha\, \mathrm{e}^{-i\epsilon X\cos\alpha} \cos(\epsilon Y \sin\alpha) \\ &= i\epsilon \sin\alpha (1 - i\epsilon X \cos\alpha) + O(\epsilon^3) \quad \text{on} \quad Y = 1,\ X < 0 \end{aligned} \tag{27}$$

and

$$\psi_A = i \sin(\epsilon Y \sin\alpha) = i\epsilon Y \sin\alpha + O(\epsilon^3) \quad \text{on} \quad X = 0,\ Y < 1. \tag{28}$$

3 Solution for the semi-infinite barrier

The solution will be presented in two main parts corresponding to the symmetric and antisymmetric potentials defined in §2. The aim is to develop perturbation expansions for the inner and outer potentials ϕ and ψ in terms of the small parameter ϵ. Superscripts in parentheses are used to indicate the order in ϵ of an expansion. So, for example, $\phi^{(n)}$ is the expansion of ϕ up to terms of order ϵ^n. When written in terms of inner coordinates and re-expanded to order ϵ^m this is written as $\phi^{(n,m)}$. Similarly, the inner solution expansion up to order ϵ^m is written $\psi^{(m)}$ and when expressed in terms of outer coordinates and re-expanded to order ϵ^n it is denoted by $\psi^{(m,n)}$. The matching principle, discussed fully by Crighton & Leppington [5], requires $\phi^{(n,m)} \equiv \psi^{(m,n)}$, term by term, when both are expressed in the same coordinates.

Before giving the full details of the formal matching procedure, it is useful to examine an informal procedure for the symmetric problem in order to guide the choice of an appropriate gauge function. One of the difficulties in applying the method of matched asymptotic expansions to problems involving 'soft' boundary conditions is the appearance of a purely logarithmic basic gauge function, of the form $(\ln\epsilon)^{-1}$, leading to series which would be of use only for extremely small values of ϵ. This problem is discussed in §6.8 of [6] and the suggested remedy is a slight change in the gauge function to one of the form $(\ln\epsilon+K)^{-1}$, for some constant K. Here, a suitable choice of K is found by considering the informal solution given next.

3.1 Informal solution of the symmetric problem

The pressure condition (10), to be applied on the barrier tip, indicates a non-zero flux across the barrier surface which in turn suggests that the principal effect on the scattered field will be source like. The leading-order outer solution of the symmetric problem satisfying (13) and (14), with ϵ set to zero, is therefore taken as

$$\phi_S = B\,H_0^{(1)}(r), \tag{29}$$

where $H_n^{(1)}$ is the Hankel function of the first kind and order n and B is a constant to be found. The leading terms in the inner expansion of this solution as $r \to 0$ are

$$\phi_S \sim B\left\{1+\frac{2i}{\pi}\left(\ln\tfrac{1}{2}r+\gamma\right)\right\}, \tag{30}$$

where γ is Euler's constant.

The solution for the inner potential may be determined with the aid of the conformal mapping

$$Z+j=\frac{2}{\pi}\left\{\ln\left[\zeta+\left(\zeta^2-1\right)^{1/2}\right]-\zeta\left(\zeta^2-1\right)^{1/2}\right\}, \tag{31}$$

where $j=\sqrt{-1}$, which maps the region exterior to the barrier in the $Z=X+jY$ plane to the upper half of the ζ plane. This mapping was used by Crighton & Leppington [5] in their solution of the hard barrier problem. For later use it is noted that

$$\zeta = j\,(\pi Z/2)^{1/2}-\tfrac{1}{4}j\,(2/\pi Z)^{1/2}\,(1+\ln 2\pi Z)+O(Z^{-3/2}\ln^2 Z) \quad \text{as} \quad |Z|\to\infty. \tag{32}$$

The leading-order inner solution must satisfy the boundary conditions (19) and (20), with ϵ set to zero, and also be source like at large distances in order to match with (30). It is easily verified that all of these conditions are satisfied by

$$\psi_S = -1 + A\,\mathrm{Re}_j \ln\left[\zeta + \left(\zeta^2 - 1\right)^{1/2}\right], \tag{33}$$

where A is to be found from the matching. As $|\zeta| \to \infty$

$$\psi_S = -1 + A\,\mathrm{Re}_j \left\{\ln 2\zeta + O(\zeta^{-2})\right\} \tag{34}$$

so that from (32), as $|Z| \to \infty$,

$$\begin{aligned} \psi_S &\sim -1 + A\,\mathrm{Re}_j \ln(2\pi Z)^{1/2} \\ &= -1 + \tfrac{1}{2}A\left\{\ln\frac{2\pi}{\epsilon} + \ln r\right\} \end{aligned} \tag{35}$$

when written in terms of the outer coordinates.

Matching the constant and $\ln r$ terms in (30) and (35) gives

$$A = \frac{4i}{\pi}B \quad \text{and} \quad B = \frac{-1}{1 + \dfrac{2i}{\pi}(\gamma - \ln(4\pi/\epsilon))}. \tag{36}$$

The denominators of A and B suggest that a suitable choice for a modified gauge function is

$$\ln\delta \equiv \frac{\pi}{2i}\left(1 + \frac{2i}{\pi}(\gamma - \ln(4\pi/\epsilon))\right) = \gamma - \frac{\pi i}{2} + \ln\frac{\epsilon}{4\pi} \tag{37}$$

so that

$$\delta = \beta^{-1}\epsilon \quad \text{where} \quad \beta = 4\pi i\,\mathrm{e}^{-\gamma}. \tag{38}$$

3.2 Formal solution of the symmetric problem

In view of the fact that the solution obtained in the previous sub-section involves an inverse power of $\ln\delta$, it is convenient to solve the problem here in terms of modified inner and outer potentials defined by

$$\hat{\psi}_S = \psi_S \ln\delta \quad \text{and} \quad \hat{\phi}_S = \phi_S \ln\delta \tag{39}$$

respectively. For the outer region the field equation is now

$$\left(\nabla^2 + 1\right)\hat{\phi}_S = 0 \tag{40}$$

and the relevant boundary condition is

$$\frac{\partial \hat{\phi}_S}{\partial y} + \beta\delta \frac{\partial^2 \hat{\phi}_S}{\partial y^2} = \beta\delta \ln\delta \ \sin^2\alpha\, \mathrm{e}^{-ix\cos\alpha} + O(\delta^2 \ln\delta) \quad \text{on} \quad y=0,\ x<0. \tag{41}$$

Similarly, the governing equations for the inner region are now

$$\left(\nabla^2 + \beta^2\delta^2\right)\hat{\psi}_S = 0 \tag{42}$$

in the flow region together with the boundary conditions

$$\frac{\partial \hat{\psi}_S}{\partial Y} = \beta^2\delta^2 \ln\delta \ \sin^2\alpha + O(\delta^3 \ln\delta) \quad \text{on} \quad Y=1,\ X<0, \tag{43}$$

and

$$\hat{\psi}_S = -\ln\delta + \tfrac{1}{2}\beta^2\delta^2 \ln\delta \ Y^2 \sin^2\alpha + O(\delta^4 \ln\delta) \quad \text{on} \quad X=0,\ Y<1. \tag{44}$$

For the leading-order inner solution the same form is adopted as in the informal solution given in the previous section, thus

$$\hat{\psi}_S^{(0)} = -\ln\delta + A_0 \,\mathrm{Re}_j \ln\left[\zeta + \left(\zeta^2 - 1\right)^{1/2}\right]. \tag{45}$$

The validity of this form will be confirmed by the subsequent matching. From (32) the outer expansion of (45) is

$$\hat{\psi}_S^{(0,0)} = -\ln\delta\left(\tfrac{1}{2}A_0 + 1\right) + \tfrac{1}{2}A_0(\ln(2\pi/\beta) + \ln r). \tag{46}$$

This source-like behaviour in the outer expansion of the inner solution suggests the leading-order outer solution

$$\hat{\phi}_S^{(0)} = B_0 H_0^{(1)}(r) \tag{47}$$

which has an inner expansion

$$\hat{\phi}_S^{(0,0)} = B_0\left\{1 + \frac{2i}{\pi}\left(\ln\tfrac{1}{2}r + \gamma\right)\right\}. \tag{48}$$

Application of the matching principle $\hat{\psi}_S^{(0,0)} \equiv \hat{\phi}_S^{(0,0)}$ gives

$$A_0 = -2 \quad \text{and} \quad B_0 = \pi i/2 \tag{49}$$

confirming the results of §3.1.

The outer expansion of the inner solution may be continued using (32) and, after some algebra, it is found that

$$\hat{\psi}_S^{(0,1)} = -\ln\frac{2\pi r}{\beta} - \delta\ln\delta\frac{\beta x}{\pi r^2} + \delta\frac{\beta}{\pi r^2}\left(x\ln\frac{2\pi r}{\beta} + y\theta\right) \tag{50}$$

which suggests that the outer solution must continue as

$$\hat{\phi}_S^{(1)} = \tfrac{1}{2}\pi i H_0^{(1)}(r) + \delta\ln\delta\,\phi_{12} + \delta\phi_2. \tag{51}$$

From (40–41), each of ϕ_{12} and ϕ_2 is a solution of the Helmholtz equation with the barrier boundary conditions

$$\frac{\partial\phi_{12}}{\partial y} = \beta\sin^2\alpha\ \mathrm{e}^{-ix\cos\alpha} \quad \text{on} \quad y=0,\ x<0 \tag{52}$$

and

$$\frac{\partial\phi_2}{\partial y} = -\tfrac{1}{2}\beta\pi i\frac{\partial^2}{\partial y^2}\left[H_0^{(1)}(r)\right] = \tfrac{1}{2}\beta\pi i\frac{H_1^{(1)}(r)}{r} \quad \text{on} \quad y=0,\ x<0 \tag{53}$$

respectively. A particular solution $\phi_{12,p}$ satisfying (52) (without the constant factor β) is given by McIver & Rawlins [7], and in particular from eqn (3.44) of that paper as $r \to 0$

$$\phi_{12,p} = \beta\frac{\alpha}{\pi i}\sin\alpha + O(r\ln r). \tag{54}$$

It is easily verified by substitution that a particular solution satisfying (53) is

$$\phi_{2,p} = \tfrac{1}{2}\beta i\left[\theta\sin\theta H_1^{(1)}(r) - \frac{\cos\theta}{r}H_0^{(1)}(r)\right]. \tag{55}$$

The outer solution to $O(\delta)$ in equation (51) is therefore taken as

$$\hat{\phi}_S^{(1)} = \tfrac{1}{2}\pi i H_0^{(1)}(r) + \delta\ln\delta\left(\phi_{12,p} + B_1 H_1^{(1)}(r)\cos\theta\right) + \delta\left(\phi_{2,p} + B_2 H_0^{(1)}(r)\right), \tag{56}$$

where any outer eigensolutions required to complete the matching with the inner solution have been included. The first order Hankel function at $O(\delta\ln\delta)$ is forced by the dipole term at the same order in (50), while the zero order Hankel function at $O(\delta)$ is forced through the constant in the inner expansion of $\phi_{12,p}$ given by (54). No other outer eigenfunctions can be matched with the inner solution and so they are excluded at this point. The inner expansion of (56) is

$$\begin{aligned}\hat{\phi}_S^{(1,1)} &= -\ln(2\pi\delta R) + \delta\ln\delta\left(\beta\frac{\alpha}{\pi i}\sin\alpha - B_1\frac{2i\cos\theta}{\pi\beta\delta R}\right)\\ &+\delta\left(\frac{\theta\sin\theta}{\pi\delta R} + \frac{\cos\theta}{\pi\delta R}\ln(2\pi\delta R) + B_2\frac{2i}{\pi}\ln(2\pi\delta R)\right)\end{aligned} \tag{57}$$

where the definition of β in (38) has been used to simplify some of the terms.

The inner expansion of the outer solution in (57) contains a source-like term at $O(\delta)$ which requires the inner solution to be continued as

$$\hat{\psi}_S^{(1)} = -\ln\delta - 2\,\mathrm{Re}_j \ln\left[\zeta + (\zeta^2-1)^{1/2}\right] + \delta\, A_1\, \mathrm{Re}_j \ln\left[\zeta + (\zeta^2-1)^{1/2}\right] \qquad (58)$$

which has the outer expansion

$$\hat{\psi}_S^{(1,1)} = -\ln\delta - \ln(2\pi R) + \frac{1}{\pi R}(\theta\sin\theta + \cos\theta.\ln(2\pi R)) + \delta\, A_1 \tfrac{1}{2}\ln(2\pi R). \qquad (59)$$

The matching principle $\hat{\psi}_S^{(1,1)} \equiv \hat{\phi}_S^{(1,1)}$ determines the unknown constants to be

$$A_1 = \frac{4i}{\pi}B_2 = \frac{2i\beta}{\pi}\alpha\sin\alpha \quad \text{and} \quad B_1 = -\tfrac{1}{2}i\beta. \qquad (60)$$

The full outer solution is therefore

$$\begin{aligned}\hat{\phi}_S^{(1)} &= \tfrac{1}{2}\pi i H_0^{(1)}(r) + \delta\ln\delta\left(\phi_{12,p} - \tfrac{1}{2}i\beta H_1^{(1)}(r)\cos\theta\right) \\ &+ \delta\left(\phi_{2,p} + \tfrac{1}{2}\beta\alpha\sin\alpha\, H_0^{(1)}(r)\right).\end{aligned} \qquad (61)$$

The far field of $\phi_{12,p}$ is given by making the substitution $\lambda = -\cos(\theta + it)$ in the integral (3.38) of McIver & Rawlins [7] and then distorting the path of integration in order to apply the method of stationary phase, see p. 31 of Noble [8] for details of the method. The result of this calculation is

$$\phi_{12,p} \sim -i\beta|\sin\alpha|\,\mathrm{e}^{-ir\cos(\theta+\alpha)}\,H[\theta+\alpha-\pi] + \frac{\beta\sin^2\alpha\, H_0^{(1)}(r)}{2(\cos\theta+\cos\alpha)} \quad \text{as} \quad r\to\infty \qquad (62)$$

for $0<\theta<\pi$, $0<\alpha<\pi$ and $\theta+\alpha \not\approx \pi$. The first term represents the possible pole capture in the deformation of the path of integration and

$$H[x] = \begin{cases} 1 & x>0 \\ 0 & x\le 0 \end{cases} \qquad (63)$$

is the Heaviside step function. Thus as $r\to\infty$

$$\begin{aligned}\phi_S^{(1)} \sim\ & \frac{\pi i}{2\ln(\epsilon/\beta)}H_0^{(1)}(r) \\ & +\tfrac{1}{2}\epsilon\left(-2i|\sin\alpha|\,\mathrm{e}^{-ir\cos(\theta+\alpha)}\,H[\theta+\alpha-\pi] + \frac{\sin^2\alpha}{\cos\theta+\cos\alpha}H_0^{(1)}(r) - iH_1^{(1)}(r)\cos\theta\right) \\ & +\frac{\epsilon i}{2\ln(\epsilon/\beta)}\left(\theta\sin\theta\, H_1^{(1)}(r) - \frac{\cos\theta}{r}H_0^{(1)}(r) - i\alpha\sin\alpha\, H_0^{(1)}(r)\right).\end{aligned} \qquad (64)$$

3.3 Formal solution of the antisymmetric problem

In this section the solution of the antisymmetric problem given in §2.2 is described. The leading-order solution $\phi_A^{(0)}$ of (23) subject to (24), with ϵ set to zero, is the scattered wave part of the Sommerfeld solution for diffraction by a thin plate, two forms for which are given in equations (2.4-5) of Crighton & Leppington [5]. According to equation (2.8) of that paper, the Sommerfeld solution has an inner expansion

$$\phi_A^{(0,1)} = S\epsilon^{1/2}R^{1/2}\sin\tfrac{1}{2}\theta + i\epsilon Y\sin\alpha \tag{65}$$

where

$$S = (2^{3/2}/\pi^{1/2})\,\mathrm{e}^{-i\pi/4}\sin\tfrac{1}{2}\alpha. \tag{66}$$

Now from (26-28) the leading-order inner solution is a harmonic function satisfying homogeneous boundary conditions and, furthermore, it is required to match with the first term in (65). The appropriate solution is found with the aid of the conformal mapping in (31-32) so that

$$\begin{aligned} \psi_A^{(\frac{1}{2})} &= \epsilon^{1/2}A_0\,\mathrm{Re}_j[\zeta^2-1]^{1/2} \\ &= \epsilon^{1/2}A_0\,\mathrm{Re}_j\left[j\left(\frac{\pi Z}{2}\right)^{1/2} + \tfrac{1}{4}j\left(\frac{2}{\pi Z}\right)^{1/2}(1-\ln 2\pi Z) + O(Z^{-3/2}\ln^2 Z)\right]. \end{aligned} \tag{67}$$

In particular

$$\psi_A^{(\frac{1}{2},0)} = \epsilon^{1/2}A_0\left[-\left(\frac{\pi}{2}\right)^{1/2}R^{1/2}\sin\tfrac{1}{2}\theta\right] \tag{68}$$

so that matching with the first term in (65) gives

$$A_0 = -\left(\frac{2}{\pi}\right)^{1/2}S. \tag{69}$$

Further terms in the outer expansion of the inner solution follow from (67) and, in terms of the outer variables,

$$\begin{aligned} \psi_A^{(\frac{1}{2},1)} &= Sr^{1/2}\sin\tfrac{1}{2}\theta - \epsilon\ln\epsilon\frac{S}{2\pi r^{1/2}}\sin\tfrac{1}{2}\theta \\ &\quad+\epsilon\frac{S}{2\pi r^{1/2}}\left[-(1-\ln 2\pi)\sin\tfrac{1}{2}\theta + \ln r.\sin\tfrac{1}{2}\theta - \theta\cos\tfrac{1}{2}\theta\right]. \end{aligned} \tag{70}$$

This suggests that the outer solution continues as

$$\phi_A^{(1)} = \phi_A^{(0)} + \epsilon\ln\epsilon\,\phi_{11} + \epsilon\phi_1 \tag{71}$$

where ϕ_{11} satisfies homogeneous boundary conditions and ϕ_1 the boundary condition

$$\frac{\partial \phi_1}{\partial y} = -\frac{\partial^2 \phi_A^{(0)}}{\partial y^2} \quad \text{on} \quad y = 0,\ x < 0. \tag{72}$$

A particular solution of the Helmholtz equation that satisfies (72) and the antisymmetry condition on $x > 0$ can be obtained by carrying out to completion the partial solution given by Crighton & Leppington [5] (for their ϕ_a with $e(\lambda) \equiv 0$ in their equation 3.11, pp. 320-321). Thus it can be shown that

$$\phi_{1,p} = -\frac{\sin\frac{1}{2}\alpha}{\sqrt{2}\,\pi^2}\int_{-\infty}^{\infty}\frac{\mathrm{e}^{-i\lambda x-(\lambda^2-1)^{1/2}y}}{(\lambda-1)^{1/2}(\lambda-\cos\alpha)}\left\{(\lambda^2-1)^{1/2}\cos^{-1}(-\lambda) - i\alpha\sin\alpha\right\}d\lambda \tag{73}$$

which has the far-field asymptotic form

$$\begin{aligned}\phi_{1,p} \;&\sim -i\sin\alpha\,\mathrm{e}^{-ir\cos(\theta+\alpha)}\,H[\theta+\alpha-\pi] \\ &\quad + \frac{\sin\frac{1}{2}\alpha\sin\frac{1}{2}\theta}{\pi(\cos\theta+\cos\alpha)}(\theta\sin\theta+\alpha\sin\alpha)H_0^{(1)}(r) \quad \text{as} \quad r\to\infty\end{aligned} \tag{74}$$

for $0 < \theta < \pi$, $0 < \alpha < \pi$ and $\theta + \alpha \not\approx \pi$, and the expansion (c.f. [5], p. 322)

$$\phi_{1,p} = b_1|x|^{-1/2}\ln|x| + b_2|x|^{-1/2} + O(|x|^{1/2}\ln|x|) \quad \text{as} \quad x\to 0 \quad \text{on} \quad \theta = \pi, \tag{75}$$

where

$$b_1 = \frac{S}{2\pi} \quad \text{and} \quad b_2 = -\frac{S}{2\pi}\left(\frac{\pi i}{2} - \gamma - \ln 2\right). \tag{76}$$

The form of the $O(\epsilon)$ outer solution is therefore

$$\phi_A^{(1)} = \phi_A^{(0)} + \epsilon\ln\epsilon\, B_0 H_{1/2}^{(1)}(r)\sin\tfrac{1}{2}\theta + \epsilon\left(\phi_{1,p} + B_1 H_{1/2}^{(1)}(r)\sin\tfrac{1}{2}\theta\right) \tag{77}$$

where appropriate eigenfunctions have been introduced to ensure matching with the inner solution. The inner expansion of this outer solution follows from (75) and on $\theta = \pi$

$$\phi_A^{(1,\frac{1}{2})} = Sr^{1/2} + \epsilon\ln\epsilon\, B_0\left[-i\left(\frac{2}{\pi r}\right)^{1/2}\right] + \epsilon\left(\frac{b_1\ln r}{r^{1/2}} + \frac{b_2}{r^{1/2}} + B_1\left[-i\left(\frac{2}{\pi r}\right)^{1/2}\right]\right). \tag{78}$$

Applying the matching principle $\psi_A^{(\frac{1}{2},1)} \equiv \phi_A^{(1,\frac{1}{2})}$ on $\theta = \pi$ gives

$$B_0 = -\frac{iS}{2^{3/2}\pi^{1/2}} \quad \text{and} \quad B_1 = \frac{iS}{2^{3/2}\pi^{1/2}}\left(\frac{\pi i}{2} - \gamma + \ln\pi - 1\right). \tag{79}$$

The far-field form of the antisymmetric solution now follows from (77) with the asymptotic form of $\phi_{1,p}$ given by (74).

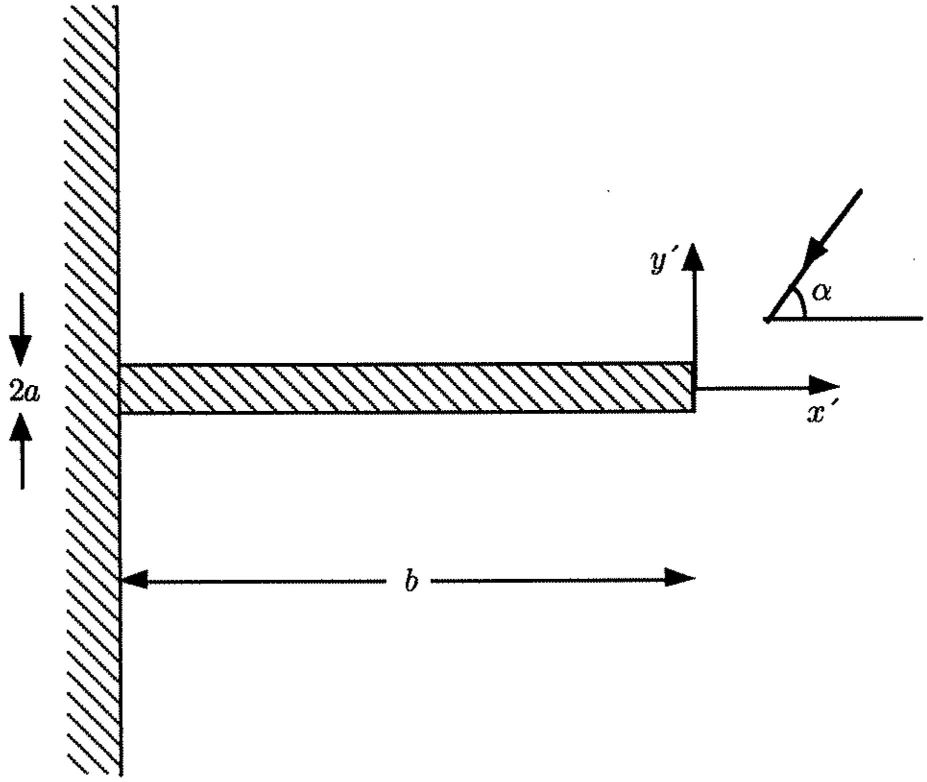

Figure 2: Definition sketch for wave scattering by finite barrier on plane.

4 Scattering by finite barrier on plane

Attention is now turned to a barrier of finite length b, again with a soft end face, that is protruding normally from an infinite plane; the geometry is illustrated in figure 2. Although the aim is to model a noise barrier standing on horizontal ground the coordinate system has been chosen for consistency with previous work [5, 7] and is essentially the same as that used in the earlier parts of the present work.

The basic formulation is very similar to that for the semi-infinite barrier given in §2. The total potential is decomposed as

$$\phi_T' = \phi_I' + \phi' \tag{80}$$

where

$$\phi_I' = 2\,\mathrm{e}^{ikb\cos\alpha}\cos[k(x'+b)\cos\alpha]\,\mathrm{e}^{-iky'\sin\alpha} \tag{81}$$

is now the incident wave together with its reflection from $x = -b$. Solutions for ϕ_T' are sought that satisfy the 'soft' condition

$$\phi'_T = 0 \quad \text{on} \quad x' = 0, \ |y'| < a \tag{82}$$

and the hard condition on the barrier sides

$$\frac{\partial \phi'_T}{\partial y'} = 0 \quad \text{on} \quad |y'| = a, \ -b < x' < 0. \tag{83}$$

There is also the additional condition of no flow through the plane on which the barrier is standing which requires

$$\frac{\partial \phi'_T}{\partial x'} = 0 \quad \text{on} \quad x' = -b, \ |y'| > a. \tag{84}$$

The geometry is still symmetric about $y' = 0$ so that the decomposition of the potential into symmetric and antisymmetric parts described in §2 is also valid for this problem. Here, due to the additional complexity, only the leading-order approximations to the far field will be determined.

4.1 Informal solution of the symmetric problem

In the symmetric problem, for brevity, the leading-order solution will be obtained using the informal procedure established for the semi-infinite barrier in §3.1. With the assumption that the barrier thickness is much less than all other length scales in the problem, the inner flow region is the same as for the semi-infinite barrier treated previously. The geometry of the outer region is now a thin barrier of *finite* length standing on a plane. In terms of the non-dimensional coordinates defined through equations (11-12), the leading-order outer solution ϕ_S is required to satisfy the (scaled) Helmholtz equation subject to the boundary conditions

$$\frac{\partial \phi_S}{\partial y} = 0 \quad \text{on} \quad y = 0, \ -\mu < x < 0 \tag{85}$$

(see equation 15) and

$$\frac{\partial \phi_S}{\partial x} = -\frac{\partial}{\partial x}\left(2\,\mathrm{e}^{i\mu\cos\alpha}\cos[(x+\mu)\cos\alpha]\cos(y\sin\alpha)\right) = 0 \quad \text{on} \quad x = -\mu \tag{86}$$

together with the symmetry condition and a radiation condition specifying outgoing waves. Here $\mu = kb$ is the scaled length of the barrier. The leading-order inner solution ψ_A is a harmonic function satisfying the boundary conditions

$$\frac{\partial \psi_S}{\partial Y} = 0 \quad \text{on} \quad Y = 0,\ X < 0 \tag{87}$$

(see equation 19) and

$$\psi_S = -2\,\mathrm{e}^{i\mu\cos\alpha}\cos[\mu\cos\alpha] \quad \text{on} \quad X = 0,\ Y < 1. \tag{88}$$

The leading order outer solution is source like at the barrier tip and the above boundary conditions are satisfied by

$$\phi_S = B(H_0^{(1)}(r) + H_0^{(1)}(r_i)) \tag{89}$$

where polar coordinates (r_i, θ_i) have been introduced that are measured from the image of the barrier tip in $x = 0$ and are defined through

$$x + 2\mu = r_i \cos\theta_i,\ \ y = r_i \sin\theta_i. \tag{90}$$

The leading terms in the inner expansion of this outer solution as $r \to 0$ are

$$\phi_S \sim B\left\{1 + \frac{2i}{\pi}\left(\ln\tfrac{1}{2}r + \gamma\right) + H_0^{(1)}(2\mu)\right\}. \tag{91}$$

The leading-order inner solution is a simple modification of the semi-infinite barrier inner solution (33) to account for the different constant appearing in the barrier-end boundary condition (88), thus

$$\psi_A = -2\,\mathrm{e}^{i\mu\cos\alpha}\cos[\mu\cos\alpha] + A\,\mathrm{Re}_j \ln\left[\zeta + \left(\zeta^2 - 1\right)^{1/2}\right] \tag{92}$$

where ζ is defined through (31). The outer expansion of this inner solution is

$$\psi_A \sim -2\,\mathrm{e}^{i\mu\cos\alpha}\cos[\mu\cos\alpha] + \tfrac{1}{2}A\left\{\ln\frac{2\pi}{\epsilon} + \ln r\right\}. \tag{93}$$

Matching (91) and (93) yields

$$A = \frac{4i}{\pi}B \quad \text{and} \quad B = \frac{-(1 + \exp(2i\mu\cos\alpha))}{1 + \frac{2i}{\pi}(\gamma - \ln(4\pi/\epsilon)) + H_0^{(1)}(2\mu)}. \tag{94}$$

4.2 Solution for the antisymmetric problem

As in §3.3, the leading-order outer antisymmetric solution is a Sommerfeld-type problem corresponding to the scattering of (the antisymmetric part of) a plane wave by a *thin* barrier. In terms of the non-dimensional coordinates defined through equations (11-12), it is required to determine solutions of the (scaled) Helmholtz equation subject to the boundary conditions

$$\begin{aligned} \frac{\partial \phi_A}{\partial y} &= -\frac{\partial}{\partial y}\left(-2i\, \mathrm{e}^{i\mu\cos\alpha}\cos[(x+\mu)\cos\alpha]\sin(y\sin\alpha)\right) \\ &= 2i\sin\alpha\, \mathrm{e}^{i\mu\cos\alpha}\cos[(x+\mu)\cos\alpha] \quad \text{on} \quad y=0,\ -\mu<x<0, \end{aligned} \tag{95}$$

and

$$\frac{\partial \phi_A}{\partial x} = 0 \quad \text{on} \quad x = -\mu \tag{96}$$

together with the antisymmetry condition and a radiation condition specifying outgoing waves.

The solution to this problem has been considered in §5 of McIver & Rawlins [7] using the Wiener-Hopf technique. The Wiener-Hopf equation was not solved exactly but an approximation for $\mu = kb >> 1$ was obtained and this will be used in the calculations here. The solution is

$$\phi_A = \frac{i}{2\pi}\left[-\,\mathrm{e}^{i2\mu\cos\alpha}J(\alpha,r,\theta) - I(\alpha,r,\theta) + \mathrm{e}^{i2\mu\cos\alpha}K(\alpha,r_i,\theta_i) + L(\alpha,r_i,\theta_i)\right], \tag{97}$$

where

$$\begin{aligned} I(\alpha,r,\theta) &= 2\pi^{1/2}e^{i\pi/4}\Big\{-\,\mathrm{e}^{-ir\cos(\theta-\alpha)}F\left[(2r)^{1/2}\cos\tfrac{1}{2}(\theta-\alpha)\right] \\ &\qquad + \mathrm{e}^{-ir\cos(\theta+\alpha)}F\left[(2r)^{1/2}\cos\tfrac{1}{2}(\theta+\alpha)\right]\Big\}, \\ J(\alpha,r,\theta) &= -2\pi^{1/2}e^{i\pi/4}\Big\{-\,\mathrm{e}^{ir\cos(\theta+\alpha)}F\left[(2r)^{1/2}\sin\tfrac{1}{2}(\theta+\alpha)\right] \\ &\qquad + \mathrm{e}^{ir\cos(\theta-\alpha)}F\left[(2r)^{1/2}\sin\tfrac{1}{2}(\theta-\alpha)\right]\Big\}, \\ K(\alpha,r,\theta) &= 2\pi^{1/2}e^{i\pi/4}\Big\{\mathrm{e}^{-ir\cos(\theta-\alpha)}F\left[(2r)^{1/2}\cos\tfrac{1}{2}(\theta-\alpha)\right] \\ &\qquad + \mathrm{e}^{-ir\cos(\theta+\alpha)}F\left[(2r)^{1/2}\cos\tfrac{1}{2}(\theta+\alpha)\right]\Big\}, \\ L(\alpha,r,\theta) &= 2\pi^{1/2}e^{i\pi/4}\Big\{\mathrm{e}^{ir\cos(\theta+\alpha)}F\left[(2r)^{1/2}\sin\tfrac{1}{2}(\theta+\alpha)\right] \\ &\qquad - \mathrm{e}^{ir\cos(\theta-\alpha)}F\left[(2r)^{1/2}\sin\tfrac{1}{2}(\theta-\alpha)\right]\Big\}. \end{aligned} \tag{98}$$

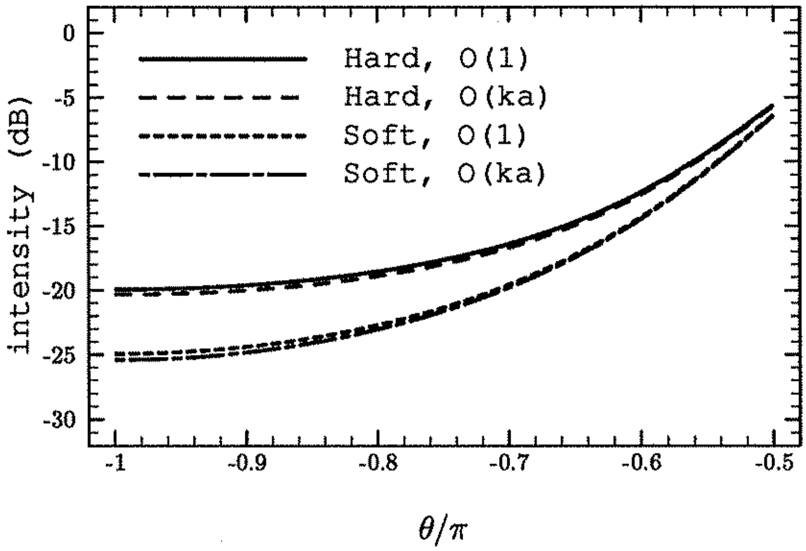

Figure 3: Semi-infinite barrier with either hard or soft end face: sound intensity v. angle θ, comparison between $O(1)$ and $O(ka)$ solutions in shadow region for $ka = 0.1$ at $r = 10\pi$.

Here

$$F[v] = \int_v^\infty e^{iu^2}\, du \tag{99}$$

is the Fresnel integral.

5 Results

All of the results presented in this section are for an angle of wave incidence $\alpha = \pi/2$, that is normal to the barrier. For the case of the semi-infinite barrier it was relatively straightforward to derive the solution up to $O(ka)$ (in this discussion terms of order $ka\,(\ln ka)^n$ are considered to be $O(ka)$, for any integer n), but for a finite length barrier standing on a plane only the $O(1)$ solution has been found. Therefore it is important to obtain some information about the expected accuracy of the $O(1)$ approximation. Figures 3 and 4 compare the two levels of approximation within the shadow region for barriers with both hard and soft end faces. Each figure displays the sound intensity, measured in decibels, based on the absolute value of the potential. For the hard end face the solution is obtained from Crighton & Leppington [5] and to order $\epsilon = ka$ the far-field form, as $r \to \infty$, is the sum of the symmetric and

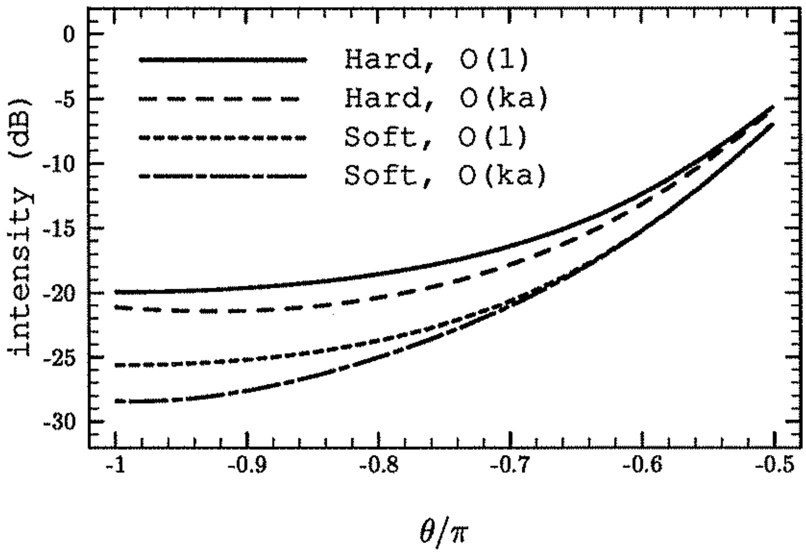

Figure 4: Semi-infinite barrier with either hard or soft end face: sound intensity v. angle θ, comparison between $O(1)$ and $O(ka)$ solutions in shadow region for $ka = 0.5$ at $r = 10\pi$.

antisymmetric potentials

$$\phi_S^{(1)} \sim \epsilon\, \tfrac{1}{2} H_0^{(1)}(r) \left\{ \frac{1 + \cos\theta\cos\alpha}{\cos\theta + \cos\alpha} \right\} \tag{100}$$

and

$$\begin{aligned} \phi_A^{(1)} \sim\ & \phi_A^{(0)} - \epsilon\ln\epsilon\, \frac{1}{\pi} \mathrm{e}^{i\pi/4} \sin\tfrac{1}{2}\alpha \sin\tfrac{1}{2}\theta H_{1/2}^{(1)}(r) \\ & +\epsilon\, \frac{1}{\pi} \sin\tfrac{1}{2}\alpha \sin\tfrac{1}{2}\theta \Big\{ \mathrm{e}^{i\pi/4} \left(1 + \ln\pi + \frac{\pi i}{2} - \gamma\right) H_{1/2}^{(1)}(r) \\ & \qquad + \frac{\theta\sin\theta + \alpha\sin\alpha}{\cos\theta + \cos\alpha} H_0^{(1)}(r) \Big\} \end{aligned} \tag{101}$$

respectively, where $\phi_A^{(0)}$ is the Sommerfeld solution for diffraction of a plane wave by a semi-infinite barrier, see for example Crighton and Leppington [5] equation (2.5). (Here and elsewhere the incident wave potential, equation (2) for the semi-infinite barrier and equation (81) for the finite barrier, is included in the calculations.) The $O(1)$ solution for the semi-infinite barrier with a hard end face is found from the limit $\epsilon \to 0$ and so is just the Sommerfeld solution. When the barrier has a soft end face the $O(ka)$ solution is the sum of the potentials in equations (64) and (77) and the $O(1)$ solution comes from the first term in each of those two equations. The agreement between the $O(1)$ and $O(ka)$ solutions for $ka = 0.1$ (figure 3) is excellent however at $ka = 0.5$ (figure 4) there are some parts of the

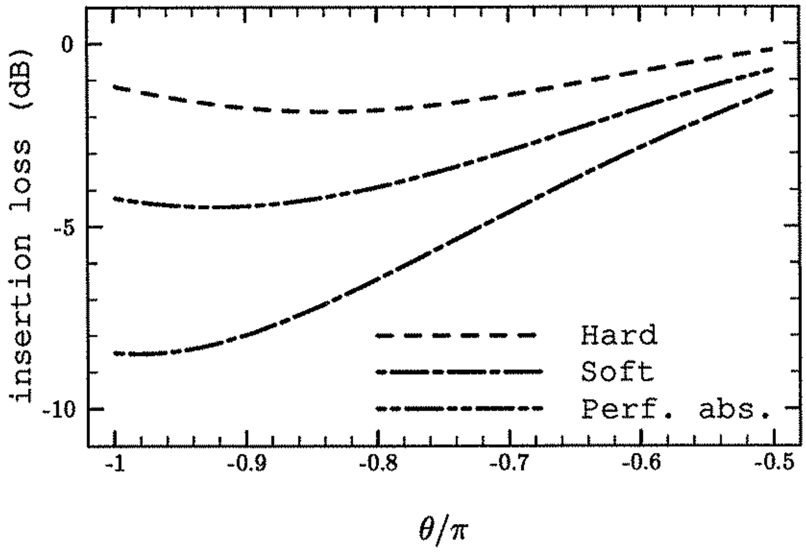

Figure 5: Semi-infinite barrier with either hard, soft or perfectly absorbent end face: insertion loss v. angle θ in shadow region for $ka = 0.5$ at $r = 10\pi$.

shadow region, particularly close to the barrier, where there are significant discrepancies. Based on these, and other, comparisons a value of about $ka = 0.5$ appears to be the upper end of the useful range of the $O(1)$ solutions for obtaining qualitative information.

The effectiveness of different types of end face in reducing the sound intensity may be measured by the so-called insertion loss. Let ϕ_{thin} denote the total potential for a rigid thin barrier, ϕ_{hard} for a thick barrier with a hard end face, and ϕ_{soft} for a thick barrier with a soft end face. In addition, results will be given for a barrier with a perfectly absorbent end face with the total potential defined by

$$\phi_{\text{perf}} = \tfrac{1}{2}\left(\phi_{\text{hard}} + \phi_{\text{soft}}\right). \tag{102}$$

Insertion losses in decibels for the hard, soft and perfectly absorbent end faces are defined as

$$20\log_{10}\left|\frac{\phi_{\text{hard}}}{\phi_{\text{thin}}}\right|, \quad 20\log_{10}\left|\frac{\phi_{\text{soft}}}{\phi_{\text{thin}}}\right| \quad \text{and} \quad 20\log_{10}\left|\frac{\phi_{\text{perf}}}{\phi_{\text{thin}}}\right| \tag{103}$$

respectively, and measure the effectiveness in sound reduction of each of the three types of end face relative to the thin barrier. In all cases the solutions are calculated to $O(ka)$. Figure 5 shows these insertions losses as a function of angle in the shadow region. The greatest losses are close to the barrier. Figure 6 shows that the insertion losses at a fixed angle in the

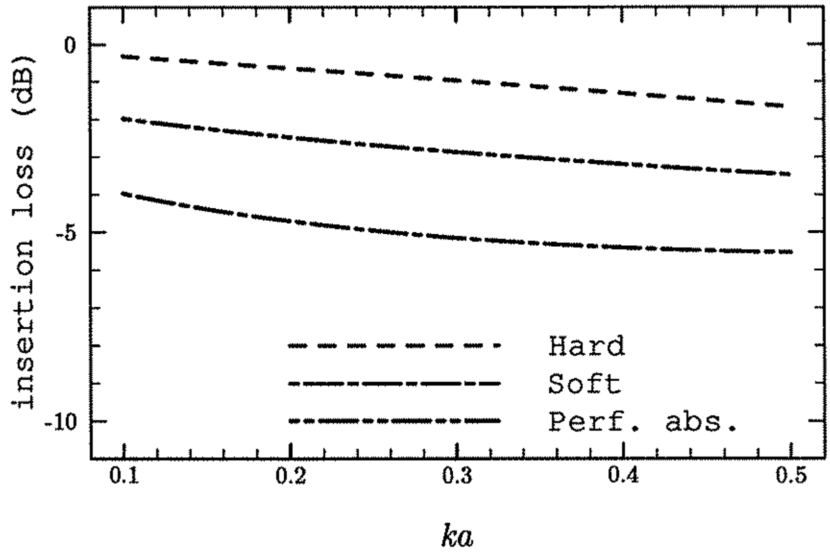

Figure 6: Semi-infinite barrier with either hard, soft or perfectly absorbent end face: insertion loss v. thickness ka at $r = 10\pi$, $\theta = -3\pi/4$.

shadow region are relatively insensitive to variation in the barrier thickness ka, at least for the range considered here.

For the finite barrier on a plane the solutions have been calculated only to $O(1)$, and at this order of approximation the solution for the hard end face is the same as the thin barrier, equation (97). This solution is illustrated in figure 7 which is a density plot of the absolute value of the potential. The incident wave (of amplitude 2, see equation 81) propagates from left to right and the barrier occupies the line $-8 < x/\pi < 0$ on $y = 0$. Dark tones indicate a region of small amplitude motion and light tones a region of high amplitude. The incident wave is reflected from the front of the barrier to give a standing wave as indicated by the alternating light and dark regions. Sound diffracted by the barrier tip enters the shadow region and is reflected from the plane giving a region of non-planar standing waves, these are of much lower amplitude than the direct reflections from the barrier face.

As only the thin barrier solution is available for the case of a hard end, insertion losses may be calculated only for the soft and perfectly absorbent end faces. A density plot of the insertion loss in the shadow region for the soft end face is given in figure 8. Over most of the region displayed there is indeed a reduction in the sound level due to the presence of the soft end face, although in small regions there is a significant enhancement of the sound levels as indicated by bright tones. These result from local minima close to zero in the motion

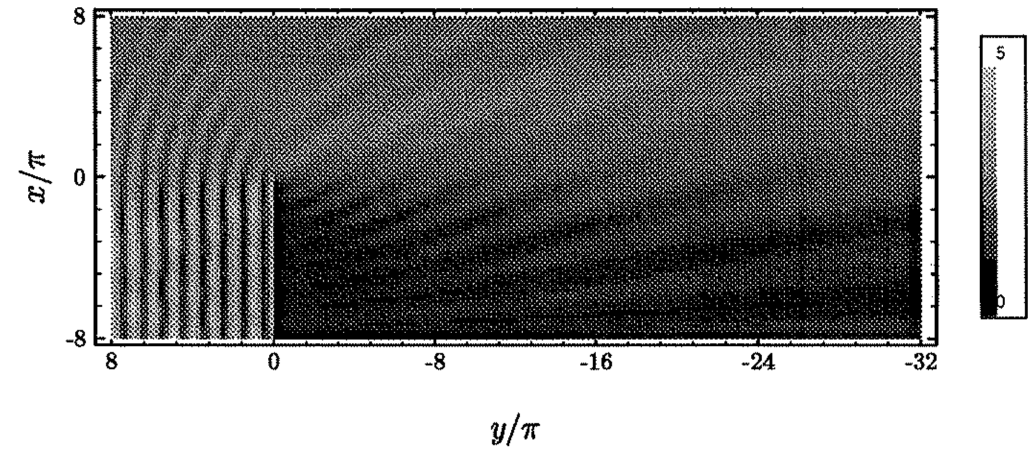

Figure 7: Finite barrier: absolute value of potential for hard barrier.

amplitudes of the thin barrier solution. A comparison of insertion losses for the soft and perfectly absorbent end faces is given in figures 9 and 10. The losses are measured in the shadow region along a line away from the barrier at a fixed height above the plane. The sharp peaks result from a local minimum in the rigid barrier solution as mentioned above. Roughly speaking, the largest reductions in noise levels due to the lined barrier end face are found close to the barrier.

References

1. G.F. Butler, "A note on improving the attenuation given by a noise barrier", *Journal of Sound and Vibration,* **32**, 367-369 (1974).

2. Z. Maekawa, "Noise reduction by screens", *Memoirs of the Faculty of Engineering Kobe University,* **11**, 29-53 (1965).

3. D.S. Jones, "The mathematical theory of noise shielding", *Progress in Aerospace Science,* **17**, 149-229 (1977).

4. A.D. Rawlins, "Diffraction of sound by a rigid screen with a soft or perfectly absorbing edge", *Journal of Sound and Vibration,* **45**, 53-67 (1976).

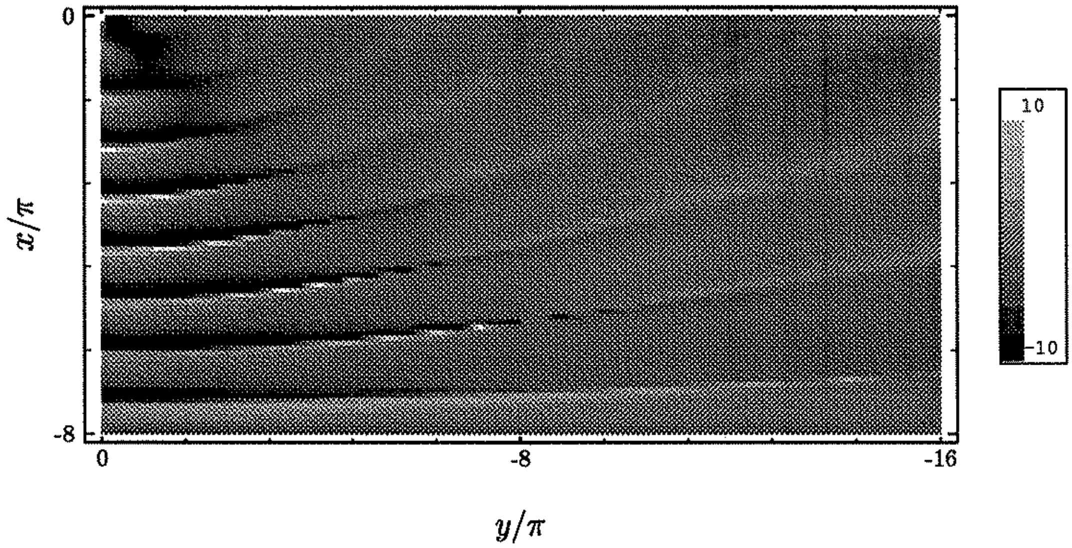

Figure 8: Finite barrier: insertion loss for barrier with soft end face, $ka = 0.5$.

5. D.G. Crighton and F.G. Leppington "Singular perturbation methods in acoustics: diffraction by a plate of finite thickness", *Proceedings of the Royal Society of London* A, **335**, 313-339 (1973).

6. D.G. Crighton, A.P. Dowling, J.E. Ffowcs Williams, M. Heckl and F.G. Leppington, *Modern Methods in Analytical Acoustics.* Springer-Verlag (1992).

7. P. McIver and A.D. Rawlins "Two-dimensional wave-scattering problems involving parallel-walled ducts", *Quarterly Journal of Mechanics and Applied Mathematics,* **46**, 89-116 (1993).

8. B. Noble, *Methods Based on the Wiener-Hopf Technique.* Pergamon (1958).

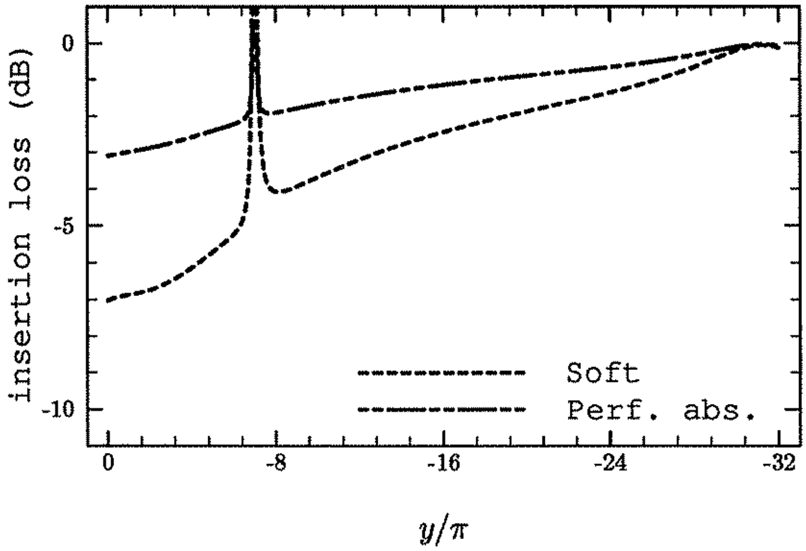

Figure 9: Finite barrier with either soft or perfectly absorbent end face: insertion loss v. distance $-y$ from barrier in shadow region at $x = -6\pi$, $ka = 0.1$.

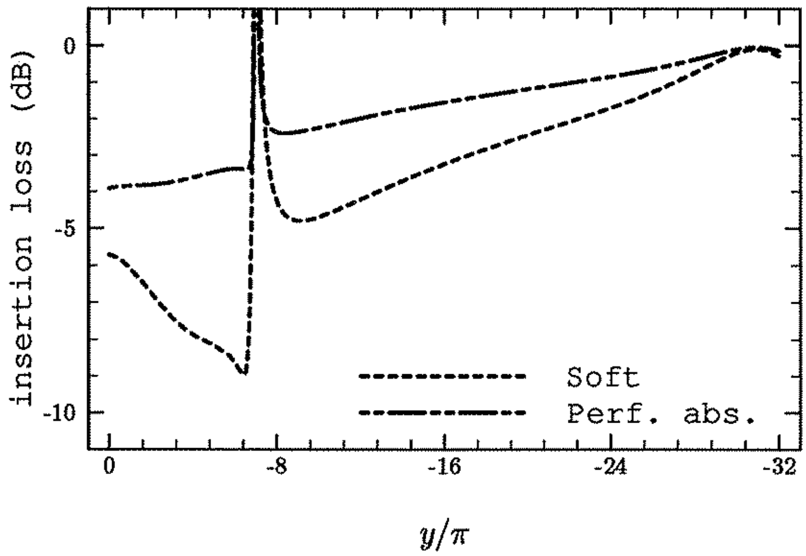

Figure 10: Finite barrier with either soft or perfectly absorbent end face: insertion loss v. distance $-y$ from barrier in shadow region at $x = -6\pi$, $ka = 0.5$.